

# AN ADVANCED MATERIAL MODEL FOR ALUMINUM SHEET FORMING AT ELEVATED TEMPERATURES

Srihari Kurukuri<sup>a,b,\*</sup>, Alexis Miroux<sup>a</sup>, Manojit Ghosh<sup>a</sup> and  
Ton van den Boogaard<sup>b</sup>

<sup>a</sup>Materials Innovation Institute(M2i)  
P.O. Box 5008, 2600 GA Delft, The Netherlands  
e-mail: s.kurukuri@m2i.nl, web page: <http://www.m2i.nl/>

<sup>b</sup>University of Twente, Faculty of Engineering Technology  
P.O. Box 207, 7500 AE Enschede, The Netherlands

**Key words:** warm forming, aluminum, deep drawing, material model, Nes hardening model

**Summary.** A physically-based material model according to Nes is used to simulate the warm forming of Al-Mg-Si sheet. This model incorporates the influence of the temperature and strain rate on the flow stress and on the hardening rate based on storage and dynamic recovery of dislocations. The effect of size and volume fraction of precipitates are considered by means of phenomenological and Orowan relations. The anisotropic behavior of the sheet is described by using the Vegter yield locus. Satisfactory results are obtained for simulation of cylindrical cup drawing.

## 1 INTRODUCTION

The excellent corrosion resistance and high strength to weight ratio offered by Al-Mg-Si sheet showed a great potential to use in automotive industry. However, aluminum sheets usually show lower room temperature formability, compared to mild steel. One way to overcome the poor formability of aluminum alloys is by temperature enhanced forming. In this process, particular parts of the blank are heated and other parts are cooled, in order to increase the formability. In order to reach an optimal temperature distribution, and to avoid numerous experiments, a numerical model for warm forming process is required. In the literature, quite a number of experimental and numerical investigations on warm forming of aluminum alloys were published<sup>1-3</sup>. Most of these investigations were performed with 5xxx series alloys. Recently researchers are inclined to 6xxx series alloys. Since, the Al-Mg-Si alloys have good corrosion resistance, and obtain high strength, controlled by the precipitates formed during the aging treatment. Therefore, the age hardening response of these alloys is very significant and hence control of precipitation during thermo-mechanical treatment is critical for attaining optimal alloy performance. Also this process is industrially more challenging and more complex in terms of microstructure-mechanical behavior relationship. In this paper, a material model for warm forming of Al-Mg-Si alloys is examined.

## 2 MATERIAL MODEL

Material models for plastic deformation that are used in process simulations commonly apply a separation of the model in a yield surface and an evolution of the yield stress (hardening). The yield surface determines the plastic flow in a multiaxial stress state, while a hardening law determines the evolution of the yield surface. The same approach is used here. For a description of the yield surface the Vegter criterion<sup>4</sup> is applied. The Vegter yield criterion is defined in principle stress space for plane stress situations meant for planar anisotropic material.

### Hardening model

The work hardening of heat treatable materials like Al-Mg-Si alloys comes mostly from the nanometer sized particles which are precipitated on certain crystallographic planes. These particles then interfere with the dislocation motion which increases the resistance to deformation and raises the strength of the alloys. Also solute atoms left in the metal matrix contribute to the hardening. The main reason for the difference in strength between tempers is due to the different sizes and density of the particles. For the naturally aged temper (T4) many of the particles do not reach the critical size (approximately 5-10 nm) and are sheared by the dislocations. For the artificially aged alloys (T6) the particles should ideally have the optimum contribution of size and density to give the maximum strength. If the particles are larger than the critical size, it is easier for the dislocations to bow round the particles by Orowan mechanism.

For modeling stress-strain curves, a temperature and strain rate sensitive physically-based work hardening model by Nes is used, predicting the evolution of the microstructure during deformation. Extensive presentations of the work hardening part of the model are given in Nes and Marthinsen<sup>5</sup>. The flow stress is assumed to be given by

$$\tau = \tau_t + \tau_p + \tau_{cl} + \alpha_1 Gb \left[ \Gamma_1 \left( \frac{q_c}{\delta \sqrt{\rho_i}} \right) \sqrt{\rho_i} + \Gamma_2 \left( \frac{q_c}{\delta \sqrt{\rho_i}} \right) \frac{q_c}{\delta} \right] + \hat{\alpha}_2 Gb \left[ \Gamma_2(0) \frac{1}{\delta} + \frac{1}{D} \right] \quad (1)$$

Where  $\tau_t$  contains all thermal contributions,  $\tau_p$  the contribution from precipitates,  $\tau_{cl}$  is a static contribution from clusters, the  $\alpha_1$ -term is the contribution from stored dislocations and the  $\hat{\alpha}_2$ -term is due to subgrains and grain boundaries.  $G$ ,  $b$ ,  $\rho_i$  and  $\delta$  have their usual meaning as shear modulus, Burgers vector, interior dislocation density (within subgrains) and subgrain size, respectively. In Eq. (1)  $\tau_t$ ,  $\rho_i$  and  $\delta$  are obtained from the Nes model while  $\tau_p$  is obtained from the Orowan relation:

$$\tau_p = \left( \frac{AGb}{1.24 \cdot 2\pi} \right) \frac{\ln(\lambda/b)}{\lambda} \quad (2)$$

Here  $A$  is a constant and  $\lambda = 0.8 \left( \sqrt{\pi/f_r} - 2 \right) r$  is the spacing between particles with average radius,  $r$ , filling a volume fraction  $f_r$ . Eq. (2) is found not to represent well the increase of the initial yield strength due to the particles. In the present work, Eq. (2) is modified by the following

$$\tau_p^{adapt} = 96.5023 + 0.2138 \cdot T - 1.1224E - 04 \cdot T^2 + \tau_p \quad (3)$$

as obtained by fitting of tensile tests at different temperatures.

### 3 SIMULATION OF CYLINDRICAL CUP DEEP DRAWING

In this section, the implemented material model is discussed in terms of a case study concerned with warm deep drawing of cylindrical cups made up of 1 mm thick AA 6016 sheet for different tempering conditions at various punch velocities and temperatures. Orthotropic symmetry was assumed for the material model. A quarter of the blank was modeled and boundary conditions were applied on the displacement degrees of freedom to represent the symmetry. The sheets were modeled with 998 discrete Kirchhoff triangular shell elements with 3 translational, 3 rotational and 1 temperature degree of freedom per node. The tools were modeled as rigid contours with a prescribed temperature. In the presented simulations the die and the blank holder were given a temperature of 250 °C, while the punch was kept at 25 °C. Simulations with the Vegter yield locus and the Nes hardening model implemented in the in-house implicit code DIEKA are performed. In the simulations a temperature dependent friction coefficient is used, with a linear relation from 0.6 to 0.12 for temperatures from 90 °C to 110 °C and constant before and after this range.

In Figure 1, the force–displacement diagrams of the punch and the thickness distributions of the cup at a depth of 64 mm are plotted for the experiments and the simulations. From the punch force–displacement curves, it can be seen that the numerical model underestimates the maximum punch force for both tempering conditions. However, this underestimation is more severe in the T6 condition. From the thickness distribution plots, it can be seen that the predicted thickness reduction in the bottom of the cup is too high with both tempering materials (T4 and T6).

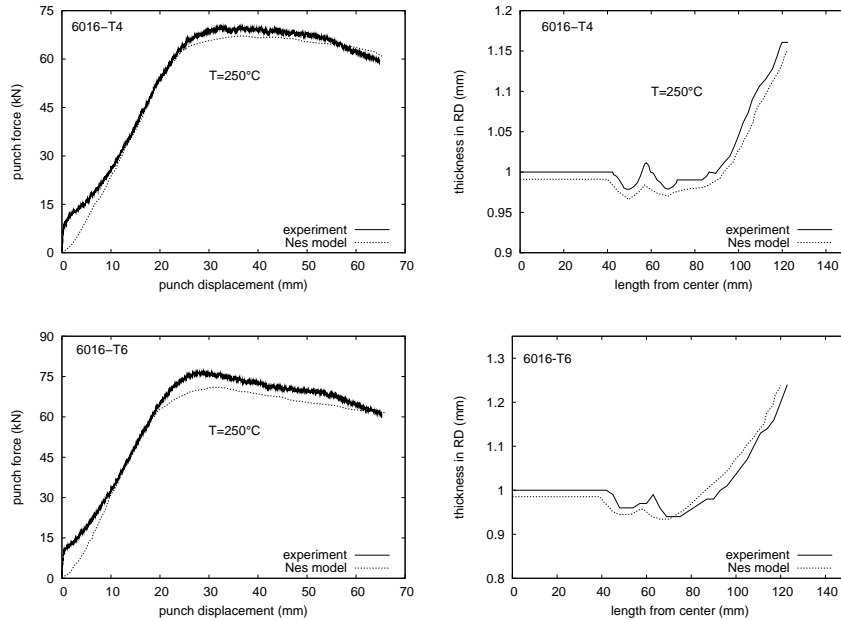


Figure 1: Deep drawing of cylindrical cup—experiments and simulations (6016-T4 and 6016-T6 alloys).

The effect of punch velocity has been investigated for AA 6016-T4 material at elevated

temperatures. The punch velocity has been varied from 13 mm/min to 78 mm/min. In the experiments, with lower punch velocity there should be more time for dynamic precipitation leading to stronger response of the material. This fact corresponds with the slightly higher force when punch velocity decreases as shown in Figure 2. Simulated punch force–displacement curves also shown the similar behavior, eventhough the evolution of dynamic precipitation is not included in the model. At higher punch velocities, the maximum punch force was underestimated. However, at lower punch velocity of 13 mm/min, the maximum punch force was slightly overestimated than the experiments due to strain rate effects in the model.

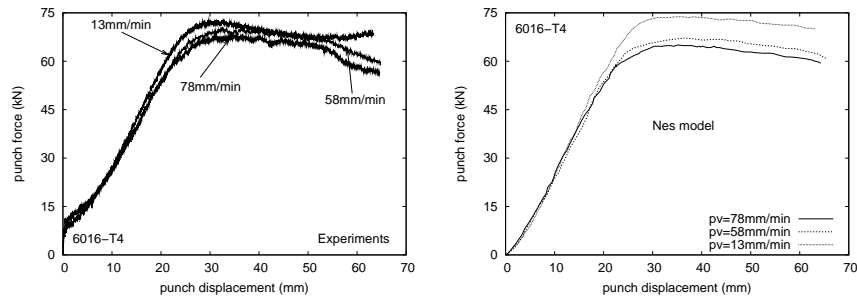


Figure 2: Deep drawing of cylindrical cup—effect of punch velocity (AA 6016-T4 alloy).

## ACKNOWLEDGEMENT

This research was carried out under the project number MC1.02106 in the framework of the Research Program of the Materials innovation institute M2i ([www.m2i.nl](http://www.m2i.nl)), the former Netherlands Institute for Metals Research. The authors are indebted to P.J. Bolt and R. Werkhoven of TNO Science and Industry for performing the warm deep drawing experiments.

## REFERENCES

- [1] P.J. Bolt, N.A.P.M. Lamboo and P.J.C.M. Rozier. Feasibility of warm Drawing of Aluminum Products. *J. Mat. Proc. Tech.*, **115**, 118–221, (2001).
- [2] A.H. van den Boogaard and J. Huétink. Simulation of aluminum sheet forming at elevated temperatures. *Comp. Methods in App. Mech. and Engrg.*, **195**, 6691–6709, (2006).
- [3] N. Abedrabbo, F. Pourboghrat and J. Carsley. Forming of AA 5182-O and AA 5754-O at elevated temperatures using coupled thermo-mechanical finite element models. *Int. J. Plast.*, **23**, 841–875, (2007).
- [4] H. Vegter and A.H. van den Boogaard. A plane stress yield function for anisotropic sheet material by interpolation of biaxial stress states. *Int. J. Plast.*, **22**, 557–580, (2006).
- [5] E. Nes and K. Marthinsen. Modeling the evolution in microstructure and properties during plastic deformation of FCC metals and alloys—an approach towards a unified model. *Mat. Sci. and Engg. A*, **322**, 176–193, (2002).